4

Power Quality Assessment in Utility Grid with Wind and Solar Energy Penetration: An Experimental Approach

This chapter presents experimental investigation of power quality (PQ) disturbances in utility grid interfaced with a wind generator and solar photovoltaic (SPV) system using Stockwell's transform. Power quality events associated with grid synchronization and outage of wind generator as well as solar PV system have been investigated. To investigate the effects of various types of loads at PCC, the same operations are carried out and associated PQ events have been detected successfully.

4.1 INTRODUCTION

Increased consumption of electricity and negative effects of fossil fuels have forced the utilities to use renewable energy (RE) sources. These sources are more suitable to environment and capable to cover deficit in demand of electrical power [Kocatepe et al., 2009]. Among various types of RE sources, the wind and solar energies have been promoted world-wide as the distributed generation (DG) sources at distribution level in recent years. Integration of these systems to the utility grid generate variable power and voltage which in turn affects the quality of power supplied to the customers [Kaddah et al., 2016]. Operational events of wind generator and SPV systems influence power quality of distribution networks which have been addressed in this work. In particular, large current variations during outage and synchronization of these generators can lead to significant voltage transients [Mohanty et al., 2013]. Power quality study of a wind farm installed in Hatay region has been presented in [Yildiz et al., 2015]. Rodriguez *et al.* [Ruiz-Rodriguez et al., 2015], investigated the voltage unbalance sensitivity for different sizes of a single-phase SPV with different penetration level in a practical distribution feeder of Spain. This helps the operators to define optimal limits. Power quality events associated with the design constraints of two different types of inverters used for integration of solar PV system to the utility grid has been detailed in [Patra et al., 2016]. Silva *et al.* [Silva et al., 2016], investigated the effect of grid connection of solar PV system on the power quality indices (PQI) of a distribution network. Plangklang *et al.* [Plangklang et al., 2016], presented a simulation based study on measurement of the PQ disturbances such as voltage sag, swell, frequency, THD and voltage ripple associated with a rooftop solar PV system integrated to the utility grid of Thailand.

Experimental set up used for investigation of the PQ disturbances associated with wind energy include a DFIG driven by wind emulator connected to an utility grid (with a series reactance connected to infinite bus). Experimental set up of solar PV system include a single-phase solar PV system integrated to an utility grid (with a series inductance connected to infinite bus) using an grid connected inverter. Power quality assessment has been carried out for the operations of outage and synchronization of wind generator and solar PV system in the presence of various types of loads at PCC. Voltage and current signals have been recorded at PCC during the various events of study. These voltage signals are analysed with the help of *S*-transform based multi-resolution to investigate the various PQ events. Proposed power quality index, maximum deviations in frequency and total harmonic distortions of voltage and current signals have been used to investigate

the effects of various types of loads on power quality.

4.2 PROPOSED *S*-TRANSFORM BASED PQ ANALYSIS METHODOLOGY

Proposed algorithm for detection of PQ disturbances is illustrated in Fig. 4.1. Power quality disturbances associated with different operations of wind generator and solar PV system in the presence of various types of loads are analysed using multi-resolution of voltage signal based on Stockwell's transform (*S*-transform). The feature plots obtained from the *S*-transform based multi-resolution analysis of the voltage include time-frequency contour (also known as *S*-contour or frequency contour), amplitude-time curve and amplitude-frequency curve. Parameters are normalized with respect to maximum values. In this work a new plot called sum absolute values curve has been introduced to enhance the performance of proposed algorithm. This curve has been obtained from the sum of absolute values of each column of the *S*-matrix obtained from *S*-transform. These feature plots are utilized to detect PQ disturbances associated with different operations. However, the total harmonic distortions in voltage signal (THD_v) and current signal (THD_i) are computed using fast Fourier transform (FFT). Variations in the power frequency are detected by continuous monitoring of system frequency. A Power quality index (*PQI*) which makes use of these features is computed in order to rate various operations with reference to quality of power as shown in Eq. (4.1).

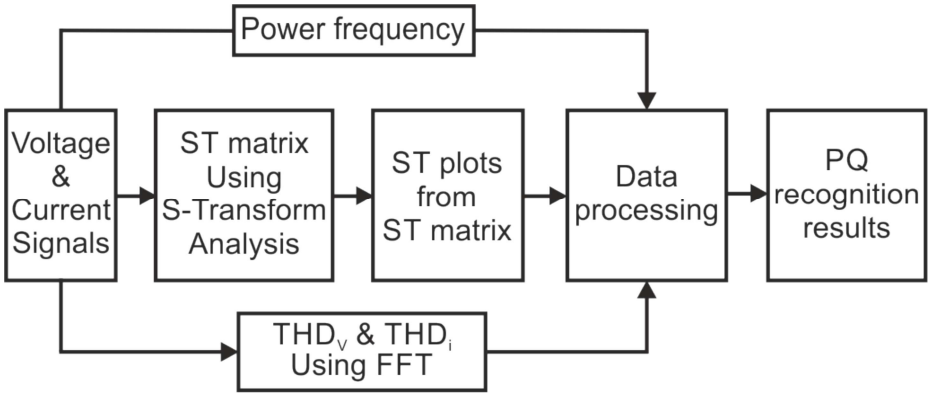

Figure 4.1 : Block scheme of PQ recognition

4.2.1 Power Quality Index

A power quality index (PQI) based on the maximum change in amplitude and sum absolute values curves, power frequency deviation, THD_v and THD_i has been proposed to rate the operational events of DFIG and solar PV system in terms of quality of power. The time durations of PQ disturbances have also been taken into consideration for the calculation of PQI. This PQ index is given by the following relation.

$$PQI = \left(\frac{\alpha_1 |\Delta A| t_1 + \beta_1 |\Delta S| t_2 + \gamma_1 |\Delta f| t_3 + \delta_1 THD_v + \sigma_1 THD_i}{5} \right) * 100 \tag{4.1}$$

where ΔA: Maximum change in amplitude curve; ΔS: Maximum change in the sum absolute values curve; Δf: Maximum change in power frequency; THD_v: Fractional total harmonics distortions of voltage; THD_i: Fractional total harmonic distortions of current; t_1, t_2 and t_3 are the time durations for which the disturbances in the amplitude, sum absolute values and power frequency persists; α_1, β_1, γ_1, δ_1 and σ_1 are the weights corresponding to amplitude, sum absolute values, frequency,

THD_v and THD_i respectively. The values of these weights have been selected unity in this study. Power quality in the utility grid is affected adversely for higher values of PQI.

4.3 EXPERIMENTAL SET-UP AND DATA ACQUISITION SYSTEM OF DFIG BASED WIND ENERGY SYSTEM

This section describes the experimental set up and data acquisition system used for power quality assessment with wind energy penetration into the utility grid. Experimental set-up for power quality measurement is shown in Fig. 4.2. Power system is an utility grid operating at voltage level of 400 V which is integrated with a wind power plant based on DFIG and wind turbine emulator. Technical specifications of the DFIG and wind turbine emulator are presented in Table 4.1. The stator of DFIG is connected to the utility grid through a 3-phase transformer with rating, 1 kVA, 400/300 V △-Y. Transformer is also fed from rotor through AC-DC-AC converter which consists of two voltage sourced converters namely Rotor side converter (*RSC*) and Grid side converter (*GSC*). A dc link capacitor which is used as an energy storage device is common element for both the converters. It provides energy buffer thereby minimizing the voltage variations. The GSC works at grid frequency whereas the RSC works at different frequencies based on wind speed. DFIG delivers power to the grid through the stator and rotor. During the super-synchronous mode of operation the power will be delivered from the rotor to the grid through converters whereas in the sub-synchronous mode the rotor will absorb power from the grid through converters. Sizing of the converters is determined by the controllable range of slip. Fig. 4.3 shows a block diagram of the DFIG.

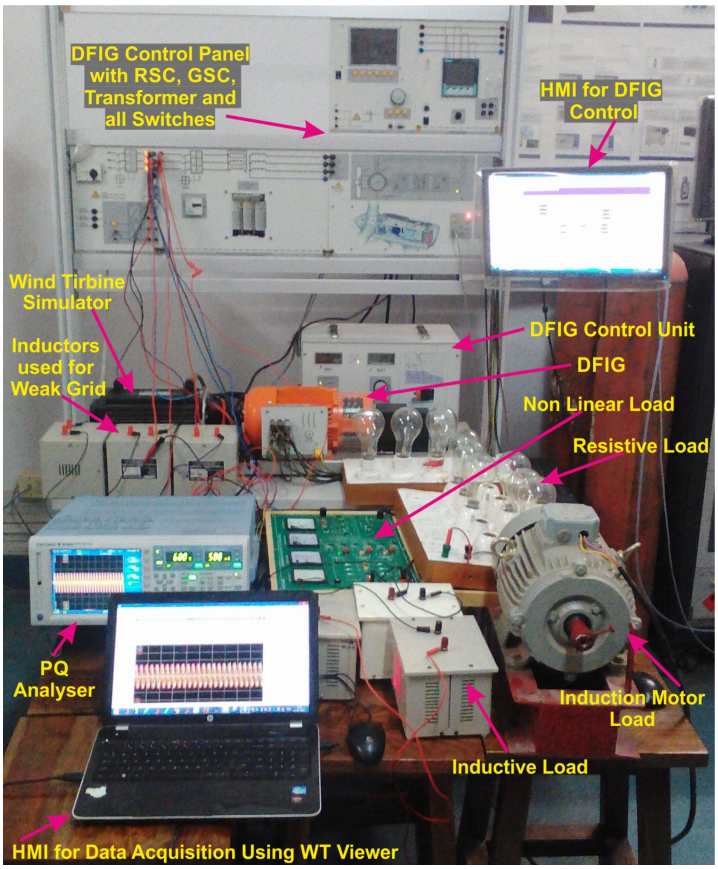

Figure 4.2 : Experimental set-up of power quality measurement with wind energy system

Data acquisition system (used for PQ assessment) is installed at PCC as shown in Fig. 4.4. Data acquisition system include a power quality analyser (WT 3000) with built in voltage and

Table 4.1 : Technical Specifications of DFIG and Wind Turbine

Parameter	Rated value
Voltage	400/230 V, 50 Hz
Current	2.0 A / 3.5 A
Speed	1400 / 1500 rpm
Power	0.8 kW
Power factor	0.75
Excitation voltage	130 VAC / 24 VDC
Excitation current	4 AAC / 11 ADC
Wind turbine maximum torque	6.7 Nm
Cut off frequency of wind turbine	70 Hz

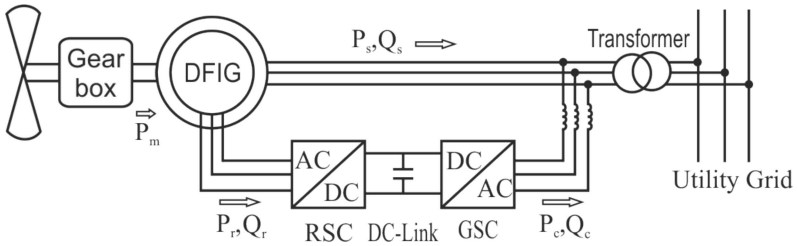

Figure 4.3 : Block diagram of doubly-fed induction generator

current transformers, Laptop computer (64-bit operating system, 4 GB RAM, Intel(I) Core(TM)i5-3230M CPU@2.60 GHz processor), WT viewer software, MATLAB software and connecting probes. A weak utility grid of short circuit capacity 7.5 kVA has been emulated by connecting an inductance of 75 mH (X_s) in series with the 3-phase supply which is integrated with a wind generator of capacity 0.8 kW. Power quality of the grid has been assessed under the events of outage and grid synchronization of DFIG in the presence of various types of loads including non-linear load. Details of the loads connected at the point of common coupling (PCC) are provided in Table 4.2. The DFIG is connected to the PCC using Grid synchronization device (*GSD*). The synchronization and outage events are emulated by closing and opening the GSD.

Table 4.2 : Loading Status at PCC with Wind Energy System

S.No.	Type of load	Load Details
1	Resistive	Y, 3-phase, 600 W per phase
2	RL Load	Y, series combination of 600 W resistive load and 0.45 H, 1.8 Ω, 330 turns inductive load in each phase.
3	Induction motor	△, 3-phase, 150 W, 50 Hz, 415 V, 1430 rpm.
4	Non-linear load	SCR based 3-phase rectifier supplying to the resistive load of capacity 25 W.

Various events associated with operations under case studies are designated as CW1-0 to CW1-4 for outage events and CW2-0 to CW2-4 for synchronization events. Table 4.3 illustrates the details of case studies.

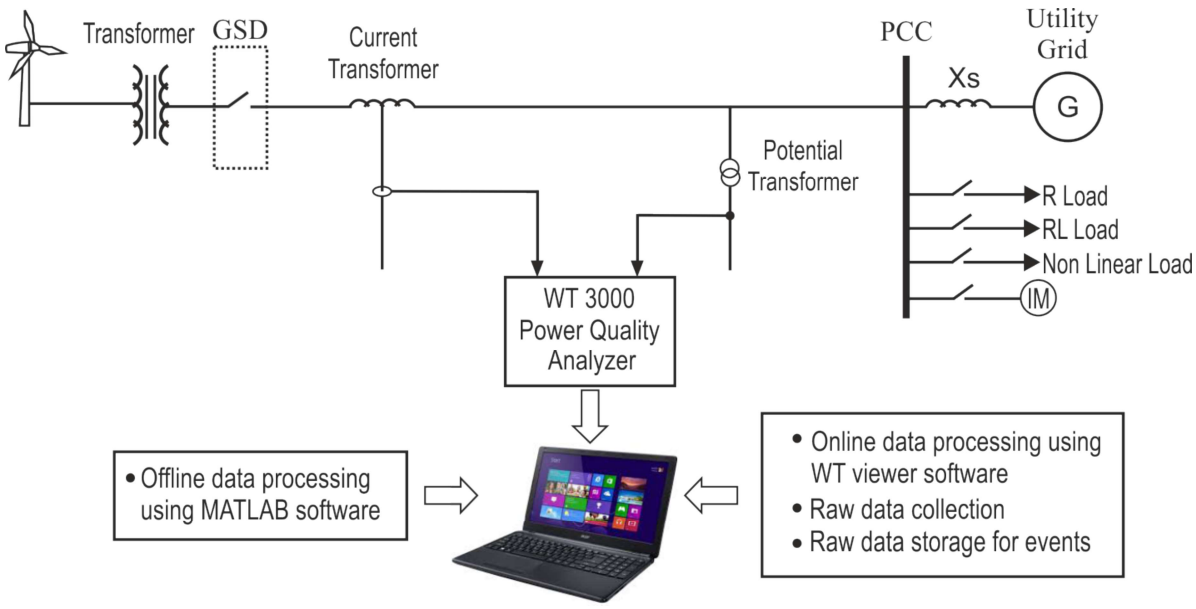

Figure 4.4 : Single line diagram of data acquisition system for power quality measurement with wind energy system

Table 4.3 : Operating Events of Wind Energy System used for PQ Measurement

Case No.	Class symbol	Event description
1	CW1-0	Outage of DFIG from utility grid in the absence of load at PCC
2	CW1-1	Outage of DFIG from utility grid in the presence of resistive load at PCC
3	CW1-2	Outage of DFIG from utility grid in the presence of RL load at PCC
4	CW1-3	Outage of DFIG from utility grid in the presence of induction motor load at PCC
5	CW1-4	Outage of DFIG from utility grid in the presence of non-linear load at PCC
6	CW2-0	Grid synchronization of DFIG in the absence of load at PCC
7	CW2-1	Grid synchronization of DFIG in the presence of resistive load at PCC
8	CW2-2	Grid synchronization of DFIG in the presence of RL load at PCC
9	CW2-3	Grid synchronization of DFIG in the presence of induction motor load at PCC
10	CW2-4	Grid synchronization of DFIG in the presence of non-linear load at PCC

4.4 POWER QUALITY ASSESSMENT WITH WIND ENERGY PENETRATION: CASE STUDIES

This section deals with the analysis of experimental results related to various disturbances caused by the outage and grid synchronization of DFIG for power quality assessment in the presence of various types of loads at PCC. The *S*-transform based plots have been compared with the respective plots of standard PQ disturbances presented in chapter 3. In order to detect the power quality disturbances, the outage and grid synchronization of DFIG have been implemented with

the help of GSD. Various case studies under different load/conditions at PCC are illustrated in the following subsections.

4.4.1 No Load at PCC

Outage of the DFIG from utility grid is performed in 3^{rd} cycle. Related *S*-transform based plots of the voltage signal at PCC are shown in Fig. 4.5 (a). A peak in the amplitude curve and sum absolute values curve indicates the presence of impulsive transient (IT). A large narrow width contour in frequency contour is also observed indicating the presence of IT for same operation. A low magnitude voltage sag can also be observed in the amplitude curve. Increase in harmonics due to outage can also be detected by high frequency ripples in frequency contour and sum absolute values curve followed by a peak. This can also be detected by increase in magnitude of the frequency amplitude curve after 0.05 normalized frequency.

The DFIG is synchronized to the utility grid at 0.04 s. Related *S*-transform based plots of voltage signal at PCC are shown in Fig. 4.5 (b). Decrease in the magnitude of amplitude curve followed by the increase in magnitude indicates the presence of voltage sag and then voltage swell due to the synchronization event. Presence of voltage variations in the amplitude curve are also observed. Low magnitude of higher order harmonics are detected in the case of synchronization which can be observed from the frequency magnitude curve with finite values other than fundamental frequency component peak. Finite values after 0.35 normalized frequency in the frequency amplitude curve indicate the presence of higher order harmonics.

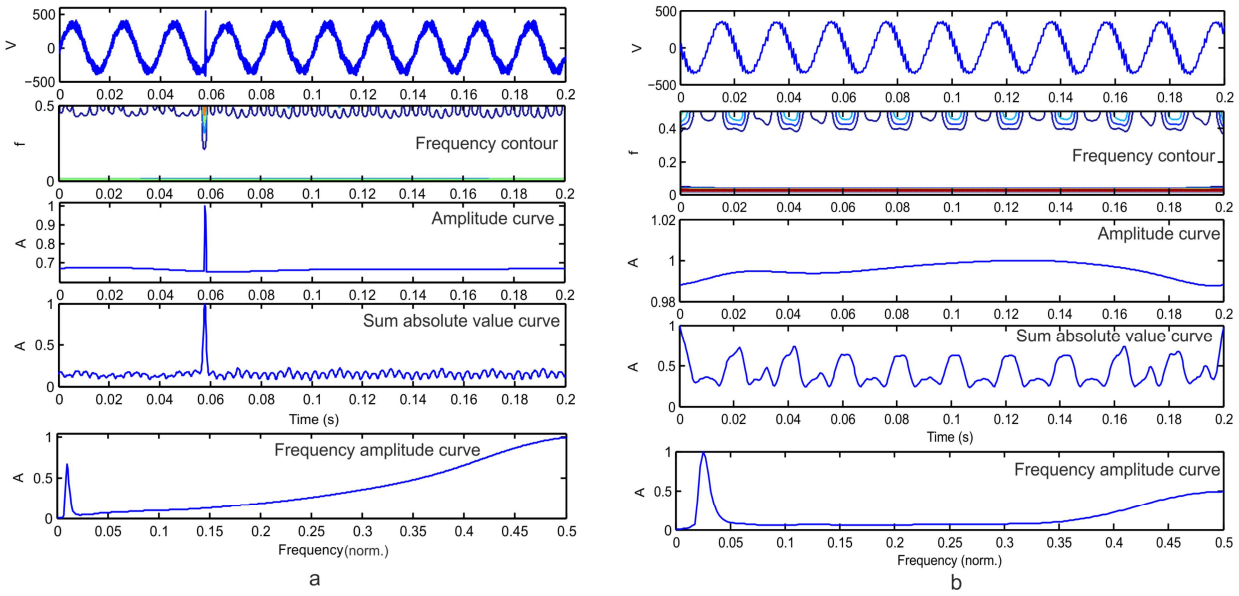

Figure 4.5 : The *S*-transform based plots of voltage signals for outage and synchronization of DFIG with weak utility grid without load at PCC (a) Voltage signal with outage and related *S*-transform based plots (b) Voltage signal with synchronization and related *S*-transform based plots

4.4.2 Resistive Load at PCC

Fig. 4.6 (a) illustrates the *S*-transform based plots related to the outage of DFIG during 5^{th} cycle in the presence of resistive load. Increase in the magnitude of higher order harmonics can be observed from increase in ripples on the surface of sum absolute values curve following the outage. Increase in the magnitude of frequency amplitude curve beyond normalized frequency 0.35 indicates presence of higher order harmonics. A voltage sag can be observed in the amplitude curve. It is also observed that low magnitude voltage variations appear due to outage.

Synchronization of the DFIG to the utility grid in the presence of resistive load at PCC is performed at 0.04 s. Related *S*-transform based plots of the voltage signal at PCC are shown in Fig. 4.6 (b). Variations in the magnitude of amplitude curve detects the voltage sag followed by low magnitude swell. These variations may cause the flicker. Finite values of frequency amplitude curve beyond normalized frequency 0.35 indicate the presence of higher order harmonics. A small value between normalized frequencies 0.05 to 0.35 in the frequency amplitude curve indicates lower order harmonics with small magnitude.

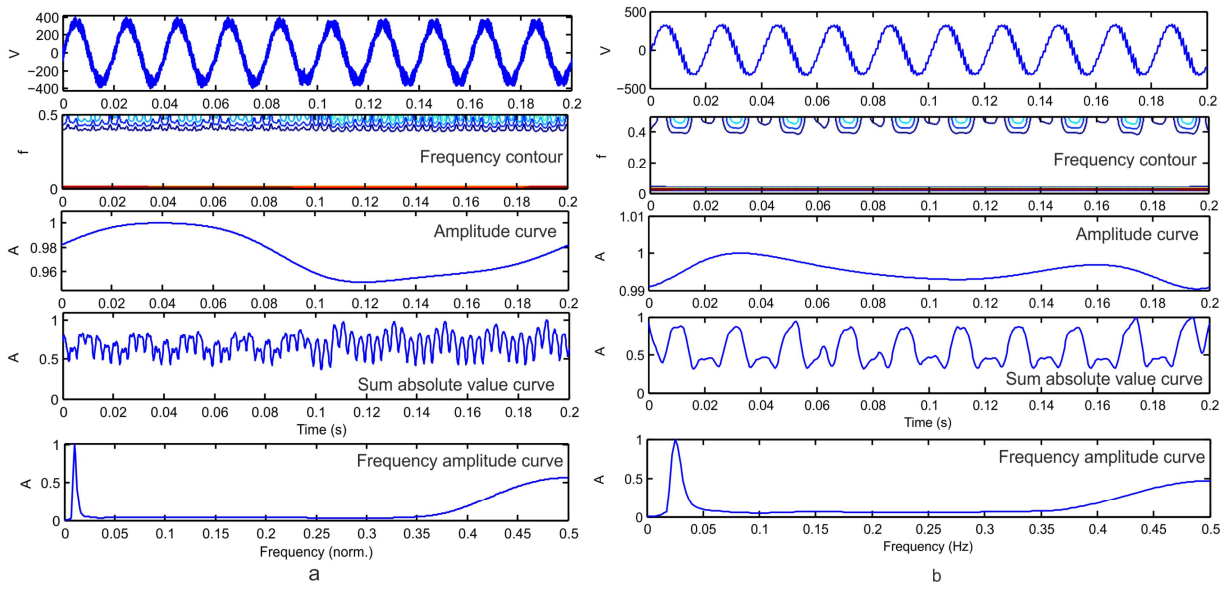

Figure 4.6 : The *S*-transform based plots of voltage signals for outage and synchronization of DFIG with weak utility grid in the presence of resistive load at PCC (a) Voltage signal with outage and related *S*-transform based plots (b) Voltage signal with synchronization and related *S*-transform based plots

4.4.3 Resistive-Inductive Load at PCC

Outage of DFIG from utility grid in the presence of resistive-inductive load at PCC is performed in the 4^{th} cycle. Fig. 4.7 (a) illustrates the related *S*-transform based plots of voltage signal at PCC. Peaks in the amplitude curve and sum absolute values curve detects the presence of IT. Presence of the IT is also validated by the presence of narrow peak upper contour at 0.062 s in the frequency contour. An isolated contour in the frequency contour plot indicates the oscillatory transient (OT). A low magnitude voltage sag is detected in the amplitude curve. Increase in the magnitude of ripples on the surface of sum absolute values curve followed by outage detect the low magnitude harmonics. Finite values beyond normalized frequency 0.35 in the frequency amplitude curve detect the higher order harmonics.

Wind generator is synchronized to the utility grid at 0.04 s in the presence of resistive-inductive load on PCC. Related *S*-transform based plots of voltage signal at PCC are shown in Fig. 4.7 (b). Isolated contours with small area in the frequency contour indicate the presence of low magnitude oscillatory transient (OT). Finite values between normalized frequencies 0.05 to 0.35 in the frequency amplitude curve also detects the OT. Increase in the magnitude of amplitude curve indicates the presence of voltage swell. Variations observed in the voltage magnitude are the source of flicker. Increased ripples on the surface of sum absolute values curve followed by synchronization indicate the presence of harmonics. Finite values of frequency amplitude curve beyond normalized frequency 0.35 indicate the higher order harmonics.

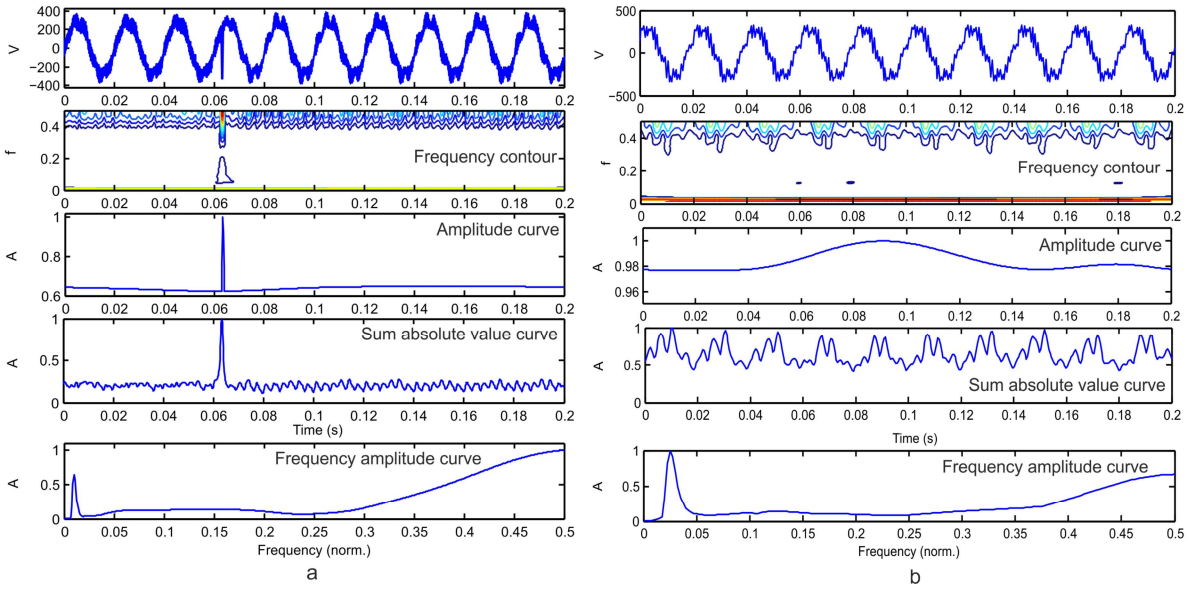

Figure 4.7 : The *S*-transform based plots of voltage signals for outage and synchronization of DFIG with weak utility grid in the presence of resistive-inductive load at PCC (a) Voltage signal with outage and related *S*-transform based plots (b) Voltage signal with synchronization and related *S*-transform based plots

4.4.4 Induction Motor Load at PCC

Fig. 4.8 (a) presents *S*-transform based plots related to the outage of DFIG from utility grid performed during 5^{th} cycle in the presence of induction motor load at PCC. Decrease in magnitude of amplitude curve detects the voltage sag. A low magnitude IT is detected by the projected contour in frequency contour plot. Peak in the sum absolute values curve and continuous finite values of the amplitude frequency curve also validate the presence of IT. Increased harmonics are detected by increase in ripples in the sum absolute values curve following the outage. Higher order harmonics can be detected by increase in the values of frequency amplitude curve beyond normalized frequency of 0.35.

The wind generator is synchronized to the utility grid at 0.04 s in the presence of induction motor load. Related *S*-transform based plots of voltage signal at PCC are shown in Fig. 4.8 (b). The voltage sag followed by voltage swell due to synchronization event are detected with the help of amplitude curve. The voltage fluctuations detected may cause flicker. Finite values of the frequency amplitude curve beyond normalized frequency 0.35 in the frequency amplitude curve indicates the higher order harmonics.

4.4.5 Non Linear Load at PCC

The non-linear load is connected at PCC. Firing angles of the Silicon controlled rectifier (*SCR*) is set such that the resistive load draws a current of 0.40 A from the rectifier at an voltage of 52 V. Outage of DFIG from utility grid in the presence of non-linear load is performed in the 4^{th} cycle. Related *S*-transform based plots of voltage signal are shown in the Fig. 4.9 (a). A voltage sag is detected in the amplitude curve by decrease in magnitude. Peaks present in the amplitude and sum absolute values curve indicate the presence of IT. A high magnitude contour in the frequency contour plot also indicates the presence of IT. A finite value in frequency amplitude plot throughout the frequency range also indicates the presence of IT. Isolated contour surrounded by the contour related to IT indicates the presence of oscillatory transient. Continuous increase in the values of

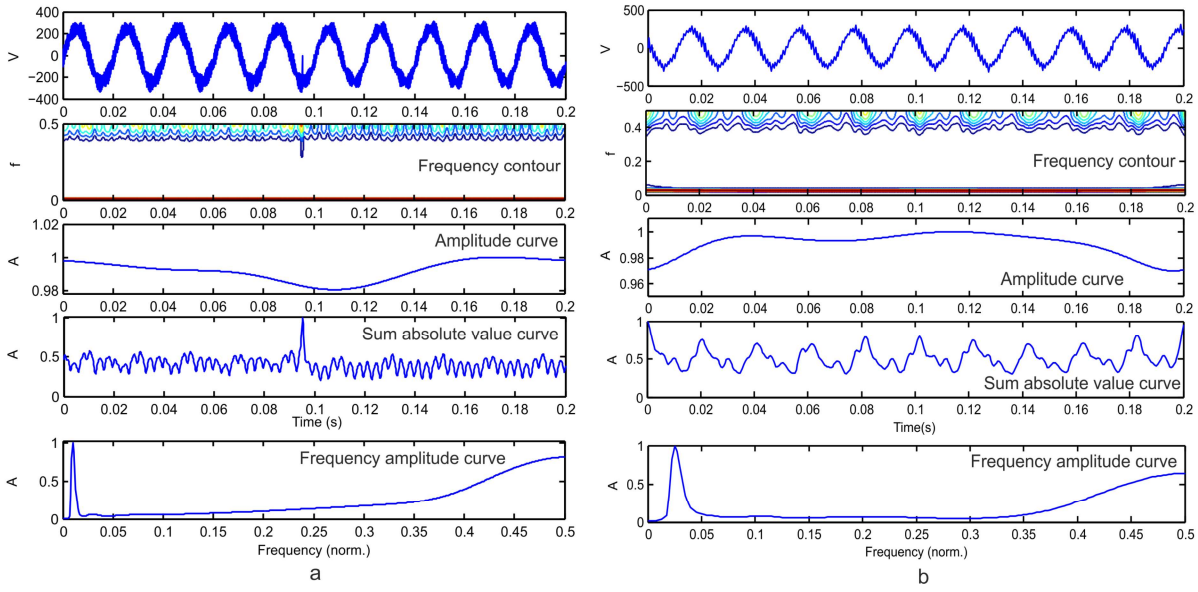

Figure 4.8 : The *S*-transform based plots of voltage signals for outage and synchronization of DFIG with weak utility grid in the presence of induction motor load at PCC (a) Voltage signal with outage and related *S*-transform based plots (b) Voltage signal with synchronization and related *S*-transform based plots

frequency amplitude plot indicates the increased magnitude of harmonics with their order.

Wind generator is synchronized to the utility grid in the presence of non-linear load at 0.04 second and respective *S*-transform based plots of voltage signal are shown in Fig. 4.9 (b). Magnitude of the amplitude curve increases just after the synchronization event indicating the presence of voltage swell. Significant values of the frequency amplitude curve beyond normalized frequency of 0.35 indicate the presence of higher order harmonics.

4.5 CASE STUDIES: COMPARISON (WIND ENERGY)

The values of total harmonic distortions in the voltage (THD_v) and current (THD_i) computed in the presence of various types of loads during synchronization and outage are presented in the Table 4.4. From this table, it can be observed that the values of THDs are low for the synchronization event as compared to the outage events. Presence of the non-linear load at PCC causes higher values of THD compared to the values due to the presence of other types of loads.

Table 4.5 presents the maximum frequency deviations and power quality index of all cases of study. It can be observed that frequency deviations are more with the synchronization event as compared to the outage event. The values of power quality index associated with synchronization event are more compared to that associated with the outage event. Thus adversed power quality is experienced in case of synchronization. Presence of the nonlinear load affects the power quality adversely compared to other types of loads.

4.6 EXPERIMENTAL SET-UP AND DATA ACQUISITION SYSTEM OF SOLAR PV SYSTEM

This section describes the experimental set up and data acquisition system used for power quality assessment with solar PV energy penetration into the utility grid. Experimental set-up for

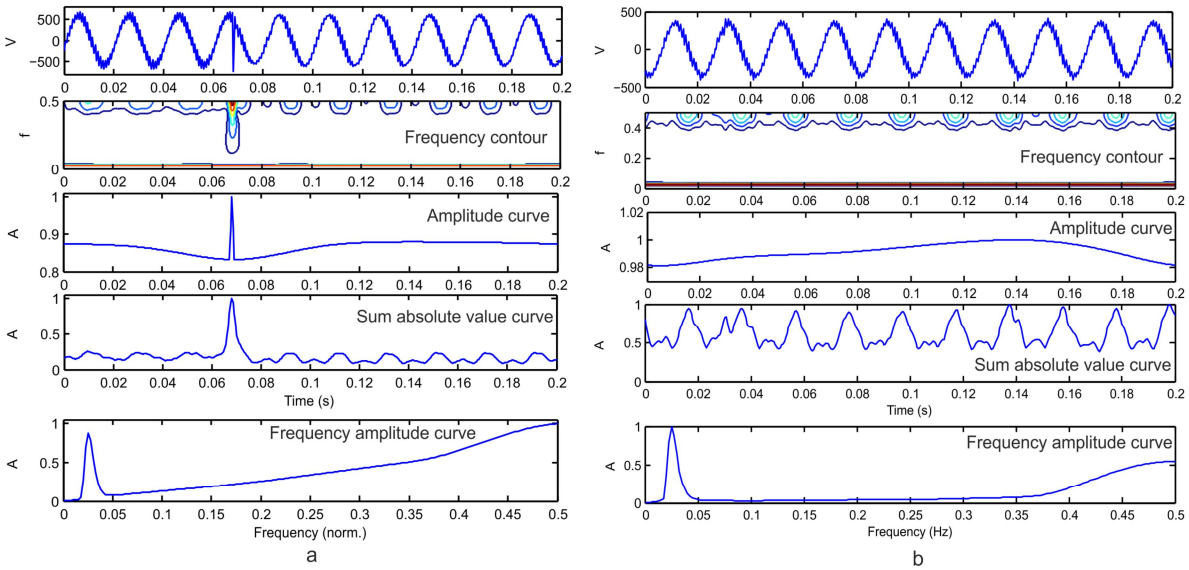

Figure 4.9 : The *S*-transform based plots of voltage signals for outage and synchronization of DFIG with weak utility grid in the presence of non-linear load at PCC (a) Voltage signal with outage and related *S*-transform based plots (b) Voltage signal with synchronization and related *S*-transform based plots

Table 4.4 : Total Harmonic Distortions of Current and Voltage with Wind Energy System

Class symbol	Total Harmonic Distortions	
	THD_v (%)	THD_i (%)
CW1-0	1.5375	1.8964
CW1-1	1.4178	1.9016
CW1-2	1.5608	2.6473
CW1-3	1.5851	2.3073
CW1-4	13.5200	26.6108
CW2-0	0.1502	1.3139
CW2-1	0.2237	1.2969
CW2-2	0.2896	1.4817
CW2-3	0.2781	1.2366
CW2-4	10.9105	17.4718

power quality measurement in the presence of solar PV system is shown in Fig. 4.10. Emulated weak utility grid consists of a 1-phase voltage source of 220 V in series with an inductor of 30 mH (short circuit rating of 5 kVA). This is integrated with a solar PV system of capacity 230 W. The solar PV system consists of a solar cell module, a joint box, a charge controller, a battery and a grid connected inverter. Characteristic parameters of the solar cell module are provided in Table 4.6. The outdoor solar PV panel supplies power to a storage battery of capacity 24 V, 55 AH through joint box and a battery charge controller. The joint box consists of a fuse and diode for the protection of solar generator and inverter. The charge controller controls the charging and discharging of battery within limits, thereby maximizing the battery lifetime. Battery is used to compensate variations in the solar PV power generation. A dc-ac converter (300 V) is used to convert dc power

Table 4.5 : Maximum Frequency Deviations and Power Quality Index with Wind Energy System

Class symbol	Maximum Frequency Deviation	Power Quality Index
CW1-0	0.0312	2.5453
CW1-1	0.0298	1.8804
CW1-2	0.0327	4.4040
CW1-3	0.0319	2.7066
CW1-4	0.0815	20.4638
CW2-0	0.0572	7.2059
CW2-1	0.0538	7.8574
CW2-2	0.0581	11.9891
CW2-3	0.0585	9.8774
CW2-4	0.1605	32.3318

generated by solar PV system to ac power and connects the same to utility grid at PCC.

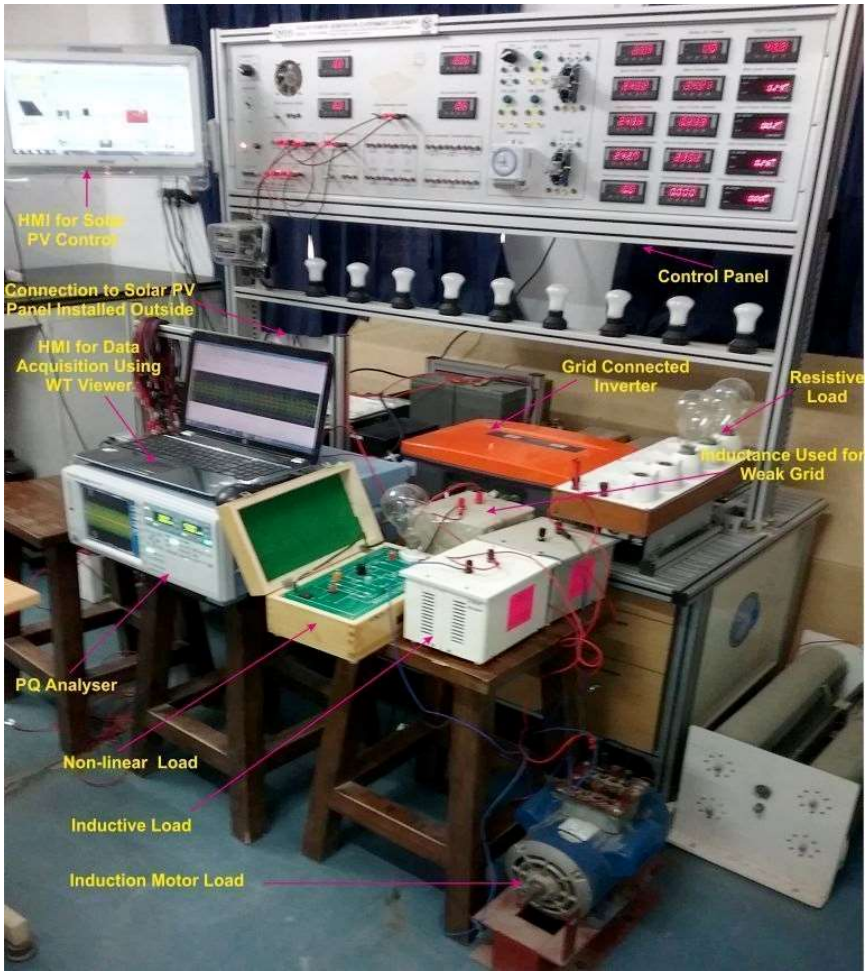

Figure 4.10 : Experimental set-up of power quality measurement with solar PV system

Data acquisition system used for PQ assessment is installed at PCC as shown in Fig. 4.11. Data acquisition system include a power quality analyser (WT 3000) with built in voltage and current transformers, Laptop computer (64-bit operating system, 4 GB RAM, Intel(I) Core(TM)i5-

Table 4.6 : Characteristic of Solar Cell Module

Parameter	Rated value
Rated power (W_p)	230 W ($\pm 3\%$)
Max. power voltage (V_{mp})	29.3 V
Max. power current (I_{mp})	7.84 A
Open circuit voltage (V_{oc})	37.1 V
Short circuit current (I_{sc})	8.42 A
Temperature coefficient of power	-0.405±0.05%/°C
Temperature coefficient of voltage	-0.312±0.015%/°C
Temperature coefficient of current	+0.075±0.015%/°C

3230M CPU@2.60 GHz processor), WT viewer software and connecting probes. Data acquisition has been carried out under the events of outage and synchronization in the presence of various types of loads at PCC. Nature of the loads connected at PCC include resistive, resistive-inductive (RL), induction motor and non-linear as detailed in Table 4.7. The solar PV system is connected at PCC using grid synchronization device (GSD). The synchronization and outage events are emulated by closing and opening the GSD.

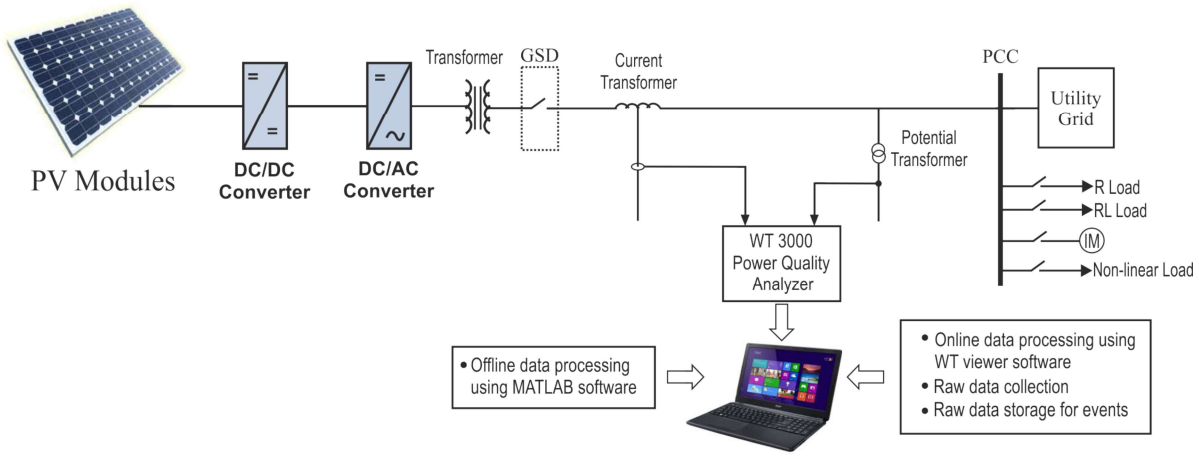

Figure 4.11 : Single line diagram of data acquisition system for power quality measurement with solar PV system

Table 4.7 : Loading Status at PCC with Solar Energy System

S.No.	Type of load	Rated value
LS1	Resistive	1-phase, 400 W
LS2	RL Load	1-phase series combination of 400 W resistive load and 0.90 H, 3.6 Ω, 660 turns inductive load.
LS3	Induction motor load	1-phase, capacitor run, 320 W, 50 Hz, 220 V, 1500 rpm.
LS4	Non-linear load	SCR based 1-phase rectifier supplying to resistive load of capacity 200 W.

Various case studies associated with the outage are designated as CS1-0 to CS1-4 whereas

those associated with synchronization are designated as CS2-0 to CS2-4 and detailed in Table 4.8.

Table 4.8 : Operating Events of Study with Solar Energy System

Case No.	Class symbol	Event description
1	CS1-0	Outage of solar PV system from utility grid in the absence of load at PCC.
2	CS1-1	Outage of solar PV system from utility grid in the presence of resistive load at PCC.
3	CS1-2	Outage of solar PV system from utility grid in the presence of RL load at PCC.
4	CS1-3	Outage of solar PV system from utility grid in the presence of induction motor load at PCC.
5	CS1-4	Outage of solar PV system from utility grid in the presence of non-linear load at PCC.
6	CS2-0	Grid synchronization of solar PV system in the absence of load at PCC.
7	CS2-1	Grid synchronization of solar PV system in the presence of resistive load at PCC.
8	CS2-2	Grid synchronization of solar PV system in the presence of RL load at PCC.
9	CS2-3	Grid synchronization of solar PV system in the presence of induction motor load at PCC.
10	CS2-4	Grid synchronization of solar PV system in the presence of non-linear load at PCC.

4.7 POWER QUALITY ASSESSMENT WITH SOLAR ENERGY PENETRATION: CASE STUDIES

This section details the results related to assessment of PQ disturbances associated with various operating events of grid connected solar PV system. The *S*-transform based plots have been compared with the respective plots of standard PQ disturbances such as voltage sag, voltage swell, momentary interruption, oscillatory transient, impulsive transient, flicker, notch, spike, harmonics and pure sine wave to effectively detect the PQ disturbances associated with the grid connected solar PV system. The synchronization and outage events of solar PV system are emulated by closing and opening the GSD as shown in Fig. 4.11. Various case studies under different load/conditions at PCC are detailed in the following subsections.

4.7.1 No Load at PCC

Outage of the solar PV system from utility grid is performed in 4^{th} cycle using GSD. Related *S*-transform based plots of voltage signal at PCC are shown in Fig. 4.12 (a). Peaks present in the amplitude and sum absolute values curves indicate the presence of impulsive transient (IT). A contour with small peak in the frequency contour also indicates the same. A low magnitude voltage sag can also be detected in the amplitude curve. Increase in the magnitude of frequency-amplitude curve after 0.30 normalized frequency indicates the presence of high frequency harmonics in the voltage signal.

The solar PV system is synchronized to utility grid in the 1^{st} cycle. The *S*-transform based plots of voltage signal are shown in Fig. 4.12 (b). Increase in magnitude of the amplitude curve indicates the voltage swell whereas the variation in amplitude also indicate the voltage fluctuations. Continuous spikes present on surface of the sum absolute values curve indicate the presence of

harmonics. Upper portion of the frequency contour also indicates the harmonics. The increase in frequency-amplitude curve beyond normalized frequency 0.35 detects the higher order harmonics.

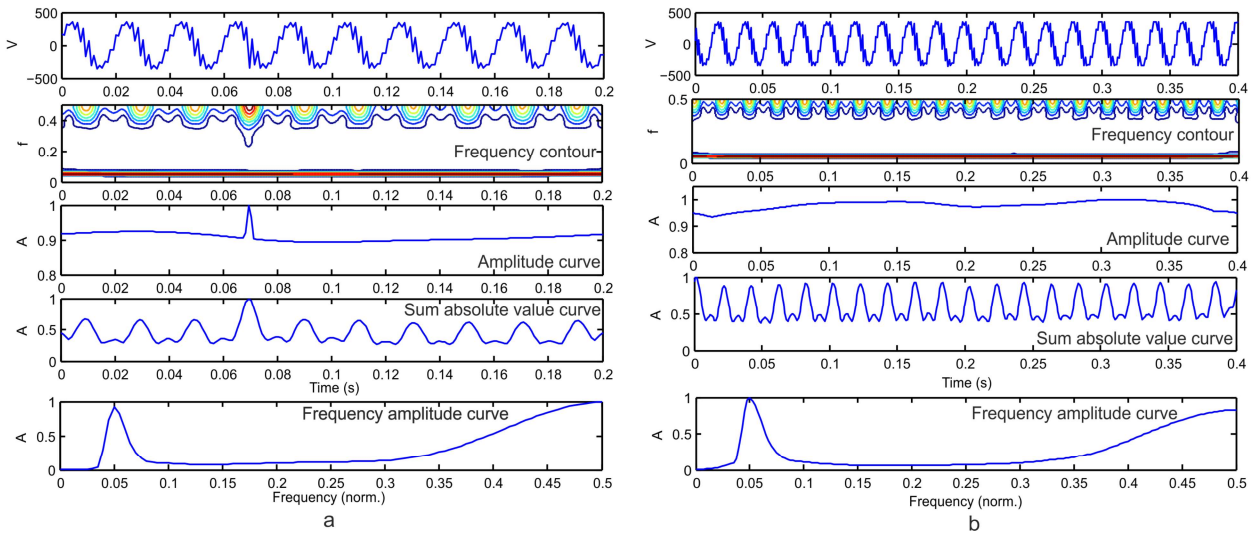

Figure 4.12 : The S-transform based plots of voltage signal for outage and synchronization of solar PV system with weak utility grid without load at PCC (a) Voltage signal with outage and related *S*-transform based plots (b) Voltage signal with synchronization and related *S*-transform based plots

4.7.2 Resistive Load at PCC

Fig. 4.13 (a) illustrates the *S*-transform based plots of voltage signal related to outage of solar PV system in the 4^{th} cycle. A voltage sag can be observed from the amplitude curve. Increase in the magnitude of frequency amplitude curve beyond normalized frequency 0.35 in frequency-amplitude curve indicates the presence of higher order harmonics.

The solar PV system is synchronized to the utility grid in 1^{st} cycle with the presence of resistive load at PCC. Respective *S*-transform based plots of voltage signal are shown in Fig. 4.13 (b). The voltage swell is observed from the amplitude curve. Sustained variations in the amplitude also indicates the presence of voltage fluctuations and flicker. Continuous spikes available on the surface of sum absolute values curve indicate the presence of harmonics. Increased values of frequency-amplitude curve beyond 0.3 normalized frequency indicate the presence of higher order harmonics.

4.7.3 Resistive-Inductive Load at PCC

Outage of solar PV system from the utility grid in the presence of RL load at PCC is carried out in 4^{th} cycle. Related *S*-transform based plots of voltage signal are illustrated in Fig. 4.14 (a). A salient contour in the frequency contour at 0.08 second indicates the presence of oscillatory transient. Decreased magnitude of amplitude curve indicates the presence of voltage sag. Change in the nature of ripples on the surface of sum absolute values curve at the instant of outage indicates the additional harmonics injected. Increasing trend in frequency-amplitude curve beyond a normalized frequency of 0.15 indicates wide range of harmonics present after the outage.

The solar PV system with RL load at PCC is synchronized to the utility grid in the 12^{th} cycle. Corresponding *S*-transform based plots of voltage signal are shown in Fig. 4.14 (b). Increased magnitude of amplitude curve indicates the presence of voltage swell followed by synchronization. Finite values of frequency-amplitude curve beyond normalized frequency 0.35 indicate the

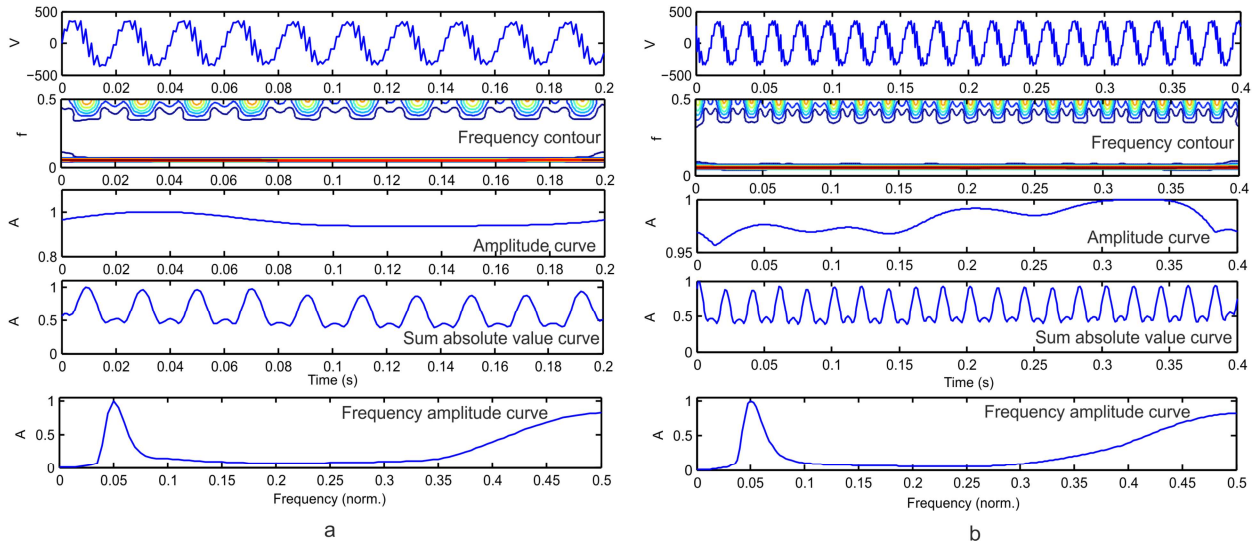

Figure 4.13 : The S-transform based plots of voltage signal for outage and synchronization of solar PV system with weak utility grid in the presence of resistive load at PCC (a) Voltage signal with outage and related *S*-transform based plots (b) Voltage signal with synchronization and related *S*-transform based plots

presence of higher order harmonics where the finite values between normalized frequencies 0.15 to 0.3 indicate the presence of lower order harmonic components.

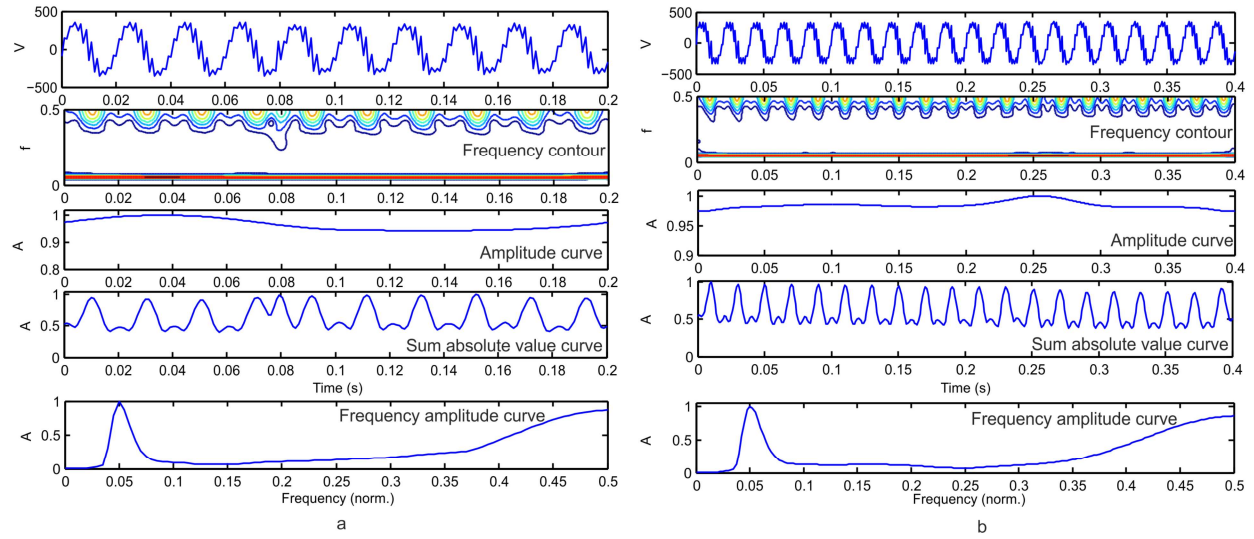

Figure 4.14 : The S-transform based plots of voltage signal for outage and synchronization of solar PV system with weak utility grid in the presence of RL load at PCC (a) Voltage signal with outage and related *S*-transform based plots (b) Voltage signal with synchronization and related *S*-transform based plots

4.7.4 Induction Motor Load at PCC

The outage of solar PV system from utility grid in the presence of induction motor load is performed in the 4^{th} cycle. Related *S*-transform based plots of voltage signal are shown in Fig. 4.15 (a). High magnitude peaks in the amplitude and sum absolute values curve indicate the presence

of impulsive transient (IT). Projected contour at 0.07 s in the frequency contour plot indicates the presence of oscillatory transient. A low magnitude voltage sag is observed in the amplitude curve. Finite values in the frequency-amplitude curve beyond 0.35 normalized frequency indicate the presence of higher order harmonics.

Fig. 4.15 (b) illustrates the *S*-transform based plots of voltage signal with grid synchronization of the solar PV system in the presence of induction motor load performed during the 2^{nd} cycle. It can be observed from the amplitude curve that voltage swell is present followed by synchronization. It also causes voltage fluctuations and flicker. Finite values of frequency-amplitude curve beyond normalized frequency 0.18 indicates the presence of wide range of harmonics and the harmonics of higher order beyond normalized frequency 0.35.

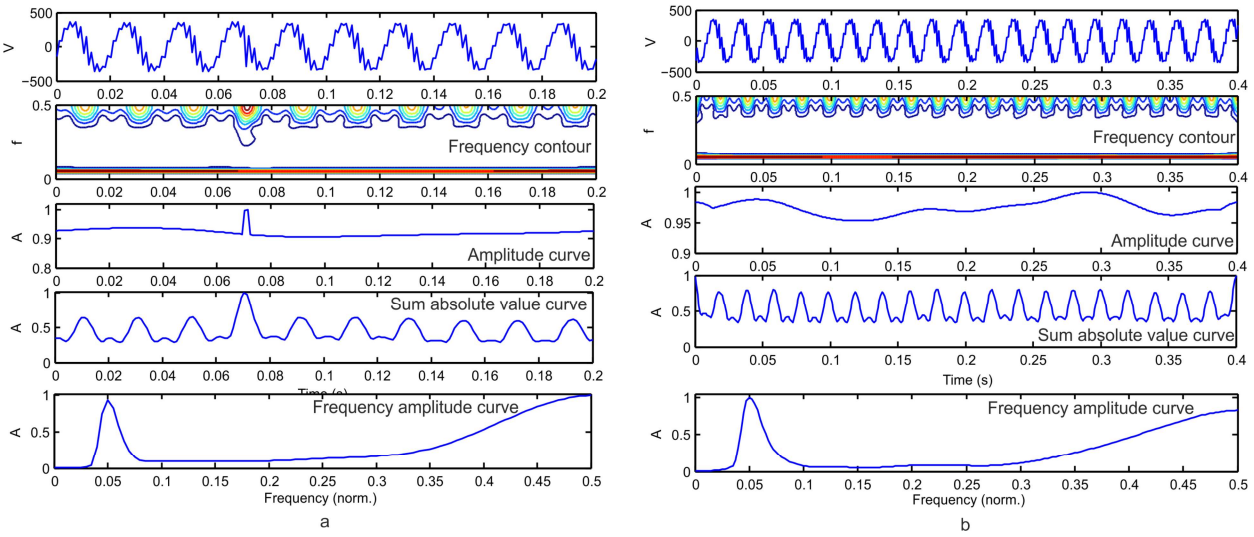

Figure 4.15 : The S-transform based plots of voltage signal for outage and synchronization of solar PV system with weak utility grid in the presence of induction motor load at PCC (a) Voltage signal with outage and related *S*-transform based plots (b) Voltage signal with synchronization and related *S*-transform based plots

4.7.5 Non-linear Load at PCC

A SCR based 1-phase converter feeding power to a resistive load of capacity 200 W is connected at PCC to investigate the power quality in the events of grid synchronization and outage of solar PV system. Outage of the solar PV system from the utility grid in the presence of non-linear load described above is performed in 3^{rd} cycle. Respective *S*-transform based plots of voltage signal are shown in Fig. 4.16 (a). A salient contour in the frequency contour indicates the presence of oscillatory transient. Decrease in the magnitude of amplitude curve indicates the presence of voltage sag for a duration of 0.02 s. A large peak in the sum absolute values curve indicates the presence of impulsive transient. A wide range of harmonics is detected by the increasing order of frequency-amplitude curve through the range of normalized frequency.

The solar PV system with non-linear load (described above) at PCC is synchronized to the utility grid in the 3^{rd} cycle. Related *S*-transform based plots of voltage signal are shown in Fig. 4.16 (b). Continuous train of circular contours in the frequency contour indicates the presence of notches. Continuous ripples in the upper portion of frequency contour indicate the harmonics. Ripples on the sum absolute values curve after the synchronization event also indicate the presence of harmonics. Increase in the magnitude of harmonics with the order is illustrated by continuous increase in the frequency amplitude curve with normalized frequency.

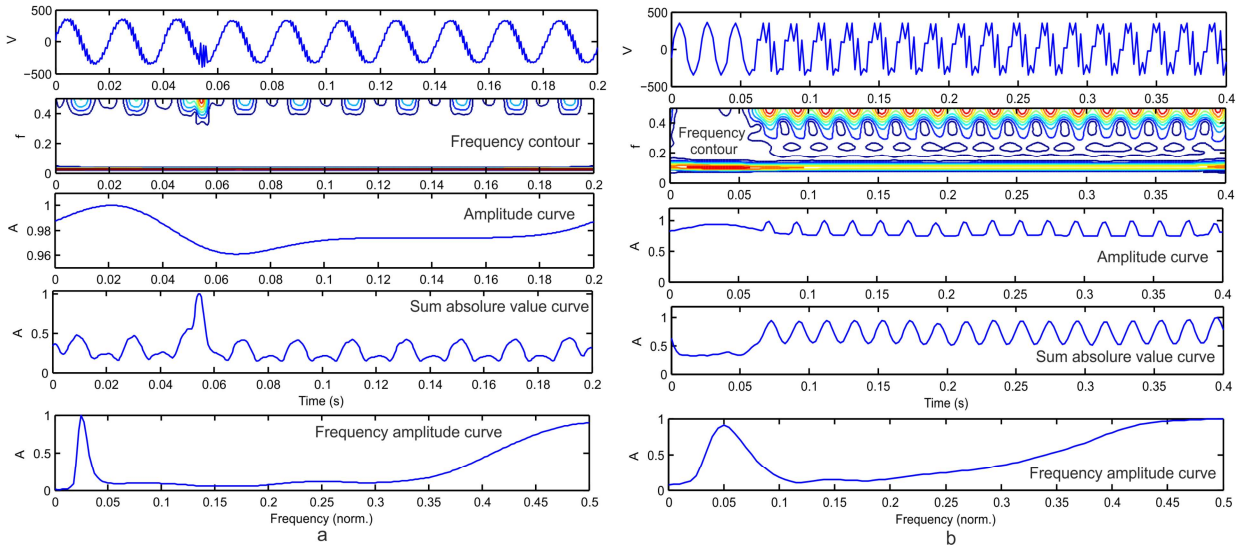

Figure 4.16 : The S-transform based plots of voltage signal for outage and synchronization of solar PV system with weak utility grid in the presence of non-linear load at PCC (a) Voltage signal with outage and related S-transform based plots (b) Voltage signal with synchronization and related S-transform based plots

4.8 CASE STUDIES: COMPARISON (SOLAR ENERGY)

Total harmonic distortions (THD) of voltage (THD_v) and current (THD_i) calculated using FFT are presented in Table 4.9. It can be observed that the values of THD_v and THD_i are more in case of outage when compared the same with that of synchronization. Highest values of THD_v and THD_i are found with non-linear load at PCC compared to other types of loads in both the events of synchronization and outage. The next level of THD are found with induction motor load at PCC. It can also be observed that the values of THD_v are less in the presence of RL load compared to the resistive load at PCC.

Table 4.9 : Total Harmonic Distortions of Current and Voltage with Solar Energy System

Nature of load	THD in voltage		THD in current	
	Outage (C1)	Synchronization (C2)	Outage (C1)	Synchronization (C2)
No load (0)	2.571	1.182	6.085	4.045
Resistive load (1)	2.805	1.194	5.980	2.957
RL load (2)	2.672	0.908	5.051	3.890
Induction motor load (3)	3.208	1.816	8.418	4.271
Non-linear load (4)	11.362	9.071	18.409	12.804

Table 4.10 presents the maximum frequency deviations and power quality indexes for outage and synchronization with different types of loads at PCC. It can be observed that the frequency deviations are more in case of synchronization compared to that associated with outage. Maximum frequency deviation in case of outage event is found with the non-linear load at PCC followed by induction motor, RL load, no load and resistive load. The same trend of frequency deviations can also be observed with the synchronization. The values of power quality indexes are more in case of synchronization compared to those associated with outage. The value of power quality index for outage cases is maximum with the non-linear load followed by induction motor load, RL load,

resistive load and no load. The same trend is observed with synchronization event.

Table 4.10 : Maximum Frequency Deviations and Power Quality Index with Solar Energy System

Nature of load	Maximum Frequency Deviation		Power Quality Index	
	Outage (CS1)	Synchronization (CS2)	Outage (CS1)	Synchronization (CS2)
No load (0)	0.037	0.287	4.3186	8.0417
Resistive load (1)	0.027	0.219	4.8670	9.9602
RL load (2)	0.042	0.312	5.2646	11.3496
Induction motor load (3)	0.048	0.369	5.6452	11.7474
Non-linear load (4)	0.183	0.816	19.5354	28.0251

4.9 CONCLUSIONS

This chapter presents experimental investigations of power quality disturbances associated with various operating scenarios of the doubly fed induction generator based wind power generation and solar PV systems integrated to weak utility grid. It is observed that the PQ disturbances such as harmonics, impulsive transient, oscillatory transient and voltage sag are associated with the outage of DFIG from the utility grid. The PQ events such as harmonics, flicker, voltage unbalance and voltage swell are associated with the synchronization of DFIG to the weak utility grid. Power quality index is high with the events of synchronization compared to the respective events of outage indicating that power quality is adversely affected with synchronization as compared to the outage. Presence of the non-linear load at PCC deteriorates the quality of supply more adversely as compared to the other types of loads. It is also observed that the PQ disturbances such as harmonics, impulsive transient, oscillatory transient, voltage sag and frequency variations are associated with the outage of solar PV system from the utility grid. PQ disturbances such as voltage swell, voltage unbalance, flicker, notches, harmonics and frequency variations are associated with the synchronization of solar PV system with the utility grid. Power quality index is high with the events of synchronization compared to the respective events of outage. Presence of the inductive components in the load affects the power quality adversely. Hence, PQ disturbances are dominant with the synchronization as compared to the outage event of solar PV system.

...